

MELT FLOW MEASUREMENT INSIDE THE KEYHOLE DURING LASER WELDING

I. Eriksson, J. Powell, A. F. H. Kaplan

Luleå University of Technology, Luleå, Sweden. www.ltu.se/tfm/produktion

Abstract

Laser keyhole welding has been in use for decades, but many of the complex mechanisms which take place within the keyhole remain poorly understood. This paper describes a streak image technique based on videos from high speed digital cameras. It is similar to the technique used in goal cameras to visualize time-dependent events. The camera's ability to acquire high speed image patterns with clear grayscale contrast has enabled us to see the melt flow on the keyhole surface. In this paper the measured flow velocity down the front of the keyhole is presented, showing a clear vertical downward motion on the keyhole front with speeds of the order of meters per second.

Keywords: Laser keyhole welding, High-speed camera, Flow measurement.

1 Introduction

Laser welding of stainless steel is an important industrial application which has been the subject of a considerable amount of theoretical simulation and experimental research [1-3]. This paper presents a new aspect of investigation into this field and, hopefully, some new insights leading towards a greater understanding of laser welding in general.

Laser welding is usually categorized into two different modes; a. conduction welding with a low power density, and b. keyhole welding, where a high power density evaporates a deep cavity or 'keyhole' in the material.

It has been demonstrated that certain laser parameters create small bumps on the keyhole front surface which experience a downward motion [4, 5]. The present authors have previously developed a streak photo technique that can measure this downward flow [6].

The main goal of this paper is to present quantitative measurements of the downward flow on the keyhole front. The flow is found to have a positive correlation to the laser power, but no correlation has been found with welding speed.

The increase in downward flow with increasing laser power resulted in the well known phenomenon of humping [1].

2 Method

This paper presents quantitative results of melt flow down the front wall of laser generated weld keyholes measured from a series of laser welds with different parameter settings.

2.1 Material

All welds were performed on 2.4mm thick stainless steel 304 (SS2333). To eliminate the influence of a gaps, only bead on plate (BOP) welds were performed. The plates were 250mm long and 100mm wide, and the length of the weld was 200mm in each case.

2.2 Laser

The laser source was a 15kW IPG fibrelaser, with a wavelength of 1070nm. The laser light was delivered by a 200 μ m delivery fibre, a 150mm collimator lens and a 300mm focusing lens. The laser beam was perpendicular to the surface with the focal point positioned 9mm below the top surface in order to produce a larger than normal keyhole. This enabled the camera to observe deep into the weld. The beam diameter on the surface of the workpiece was measured with a Prometec Laserscope UFF100, and at 800W laser power the 4-sigma diameter was 0,9mm. The beam profile was close to Gaussian (**Fig 1**).

Although the experiments employed laser powers up to 15kW, any thermal focusing problems were minimised due to the short welding time (1 to 4 seconds).

2.3 Setup

The flow measurements were made with the help of a high speed camera. The keyhole was viewed from behind at a 45 degree inclination (**Fig 2**). A Photron SA1 camera with 200mm Nikkor lens and 46mm distance rings gave a field of view of 3mm from a distance of 400mm. To be able to capture 180 000 fps with a 1 μ s shutter time, an image size of 128x128 pixels was chosen.

In this setup the laser beam and the camera remained stationary while

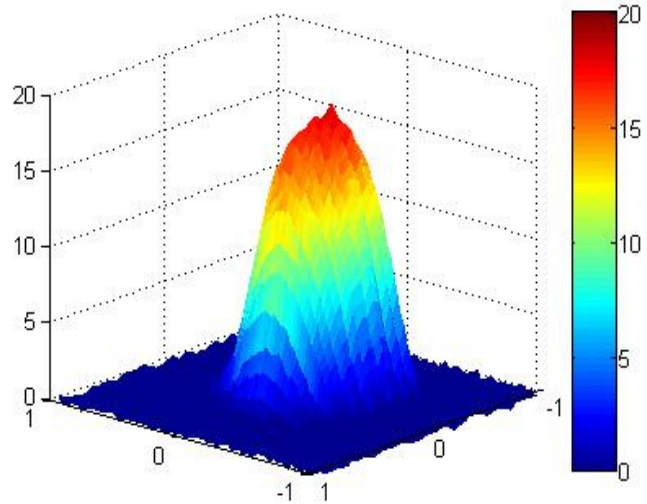


Fig 1. Beam profile on top surface at 800W laser power with -9mm focus position

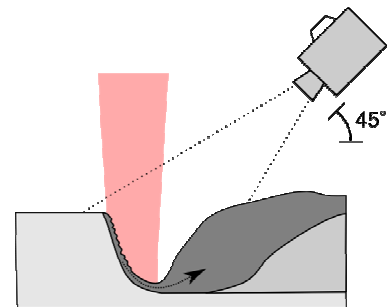


Fig 2. Schematic setup, side view of keyhole and melt pool

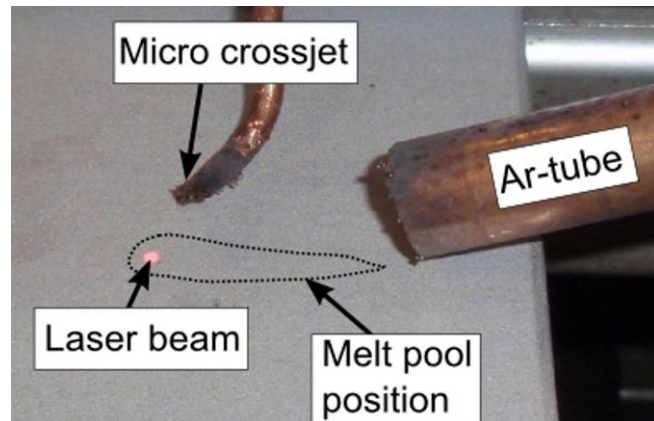


Fig 3. Position of micro crossjet

the welded plate moved. To minimize the influence of the laser induced plume [8, 9, 2] a micro cross-jet was placed a few mm above the keyhole (**Fig 3**). The cross-jet was a flattened copper tube blowing compressed air at a high velocity, parallel to the workpiece surface. A laminar flow of argon covered the melt pool from the rear.

2.4 Streak image technique

After capturing a high speed video of 4000 frames, the velocity of flow in the video was calculated using a streak photo technique [6]. From each frame (**Fig 4**) one line of pixels are extracted, and then these individual pixel lines are stacked as columns next to each other to create a streak image (**Fig 5**). In this sort of image a bright spot on the surface of the melt is tracked as it moves down the keyhole front. The vertical axis of the streak image represents distance travelled down the keyhole front – from top to bottom. The horizontal axis of the streak image represents time. So a bright dot moving down the keyhole front looks like an inclined line on the streak image – and the closer to vertical the streak is, the faster the dot was moving.

The images from the high speed camera were calibrated to a mm scale laid flat on the workpiece surface. Because of the 45 degree inclination of the camera this calibration only gives an accurate distance (velocity) reading if the front keyhole wall is vertical or horizontal. In fact the keyhole face will be somewhere between these two extremes – becoming less vertical as welding speeds are increased [10]. In the worst case scenario of a

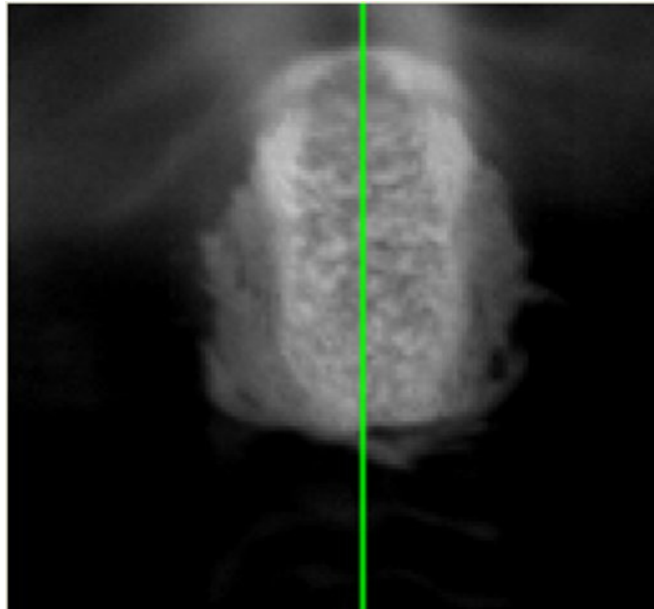


Fig 4. A single frame from high speed video. The line are pixels extracted from the image.

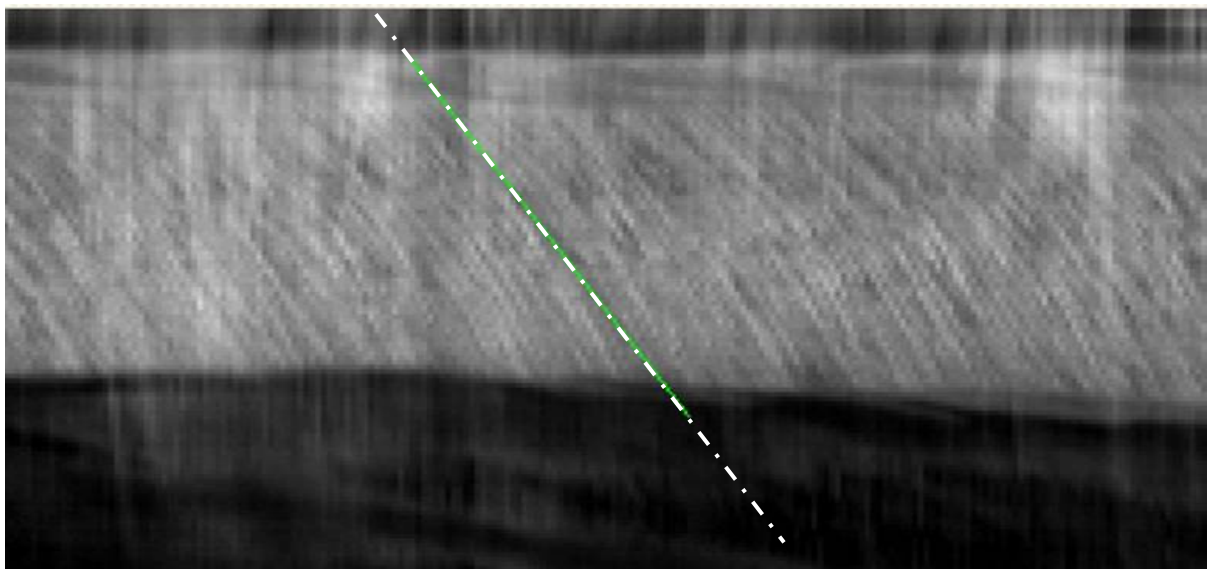


Fig 5. Streak image from 255 frames Dashed line represents 8,4m/s velocity

45 degree inclination of the keyhole front wall, the distances (and thus velocities) involved will be overestimated by 41.4%.

In the streak image, motion at a constant speed will show up as inclined straight lines. In **Fig 5** a slight acceleration of the melt is seen as it moves down the keyhole front, with a mean velocity of ~8,4m/s.

2.5 Fourier transform analysis

Measurement of the angles of streaks in images like the one in **Fig 5** gives a quick estimation of the velocities involved in the downward flow. But to achieve a more accurate value of the velocity distribution a 2d-FFT (**equ. (1)**) can be utilized.

Because the pixels in the streak image are square, the 2D-FFT was scaled to a square image of 512 x 512 pixels. (**Fig 6**) This 2D-FFT plot shows the frequency content of the streak image. Brighter areas represent a higher content of a particular frequency.

$$F(u, v) = \frac{1}{MN} \sum_{x=0}^M \sum_{y=0}^N f(x, y) e^{-i2\pi \left(\frac{ux}{M} + \frac{vy}{N} \right)} \quad (1)$$

In the FFT image low frequencies are represented towards the centre and high frequency towards the edges of the image.

The velocity lines in the streak image will appear as a bright areas perpendicular to the angle of the lines in the FFT image. As seen in **Fig 6** there is not a single downward velocity, but more of a velocity distribution. A manual estimation of the most dominant velocity was made by placing a line in the FFT-image. The velocity could then be calculated from the angle of the line. In **Fig 6** the angle of inclination of this straight line represents an average melt flow speed of 8.4 m/s.

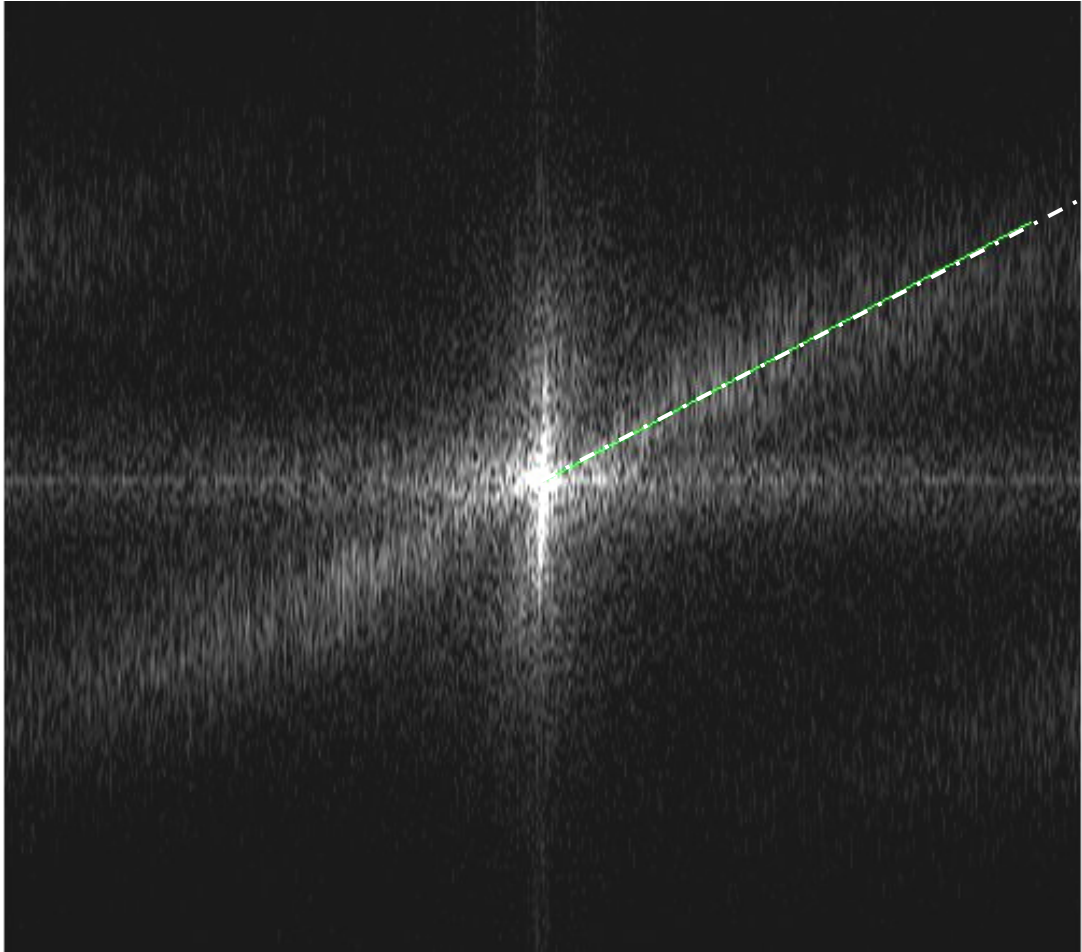


*Fig 6. 2d-FFT of a 4000 line streak image.
Dashed line represents 8,4m/s*

3 Results

3.1 Parameter influence on downward flow.

The results from the 2d-FFT velocity estimation of a wide range of welds are shown in **Fig 7 (a-c)**. The most dominant velocity* is presented in the graphs, but it is interesting to note that the maximum downwards velocity in the streak images was estimated to be as high as 25m/s for 15kW laser power. (*this is the most common velocity – not the average velocity).

In the three graphs below, results from 21 different welds are plotted with different parameters on the X-axis. No measurable downward flow was found for welding speeds lower than 50mm/s.

At 5kW laser power there was no significant change in the measured melt velocity even when changing the weld speed from 50mm/s to 200mm/s (3/min to 12m/min). At 15kW and 10kW there was a decrease in downwards flow velocity at lower speeds. At speeds below 100mm/s, the 10kW and 15kW laser powers completely penetrated the 2,4mm plate, spraying molten metal from the bottom of the ‘weld’ and leaving only a cut kerf.

Fig 7b and 7c demonstrate that, although there is a direct correlation between melt flow velocity and laser power, this is not linked to a correlation between melt speed and line energy.

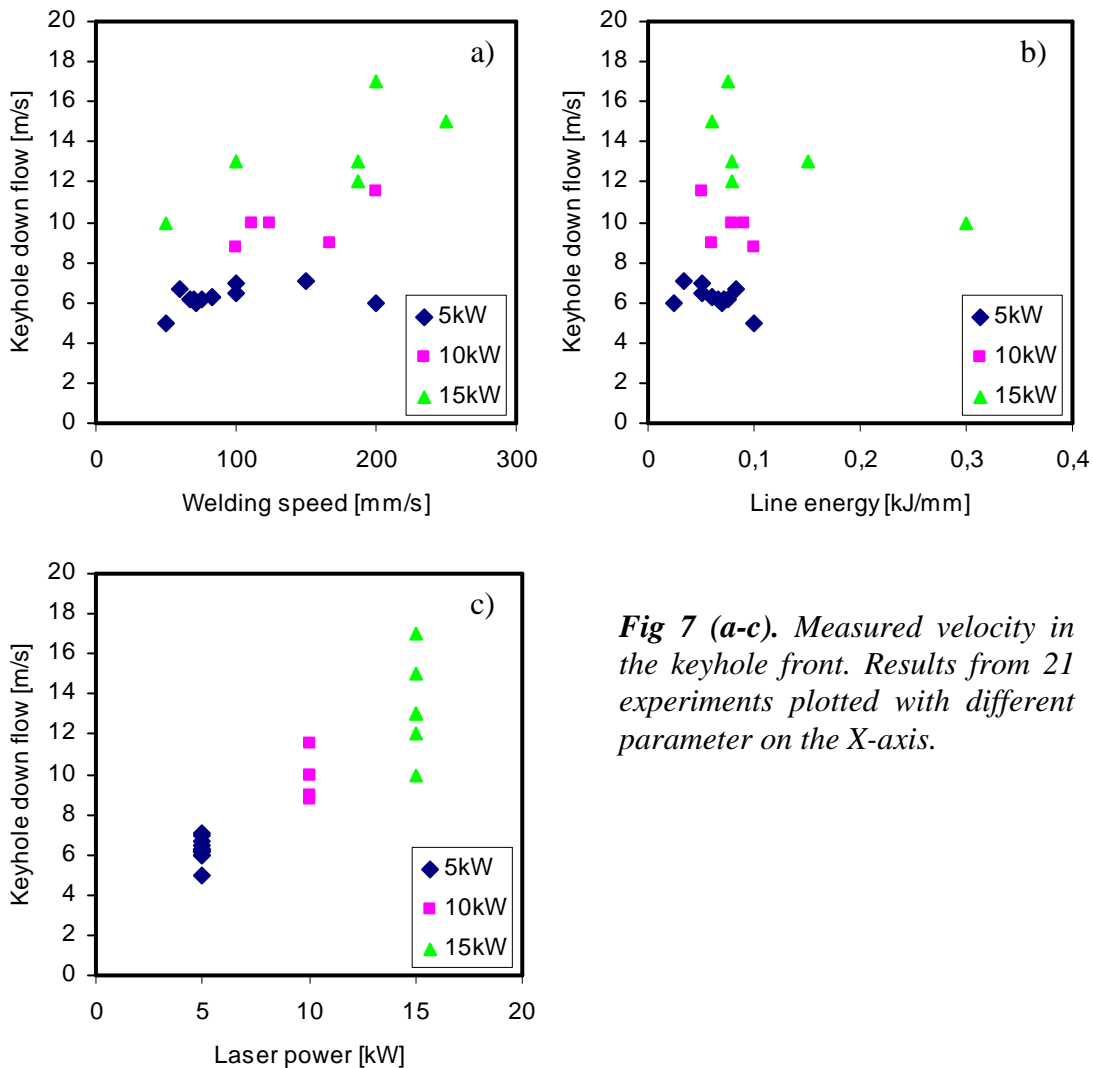


Fig 7 (a-c). Measured velocity in the keyhole front. Results from 21 experiments plotted with different parameter on the X-axis.

3.2 Welds with constant line energy

A set of welds with constant line energy of 0,06kJ/mm was carried out; at this line energy the laser power in kW is equal to the welding speed in m/min. The weld depth measured from etched cross cuts was almost constant. (**Fig 8**)

The weld depth was close enough to the root side to create some change of colour. This colour change showed a periodical behaviour in the welds with a laser power of 8-10kW, in all other welds the colour change was almost constant over the entire welding length.

A longitudinal section along the weld produced with 9kW laser power showed a sinusoidal weld depth variation. (**Fig 9**) The weld depth varied between 1,65mm and 1,9mm. The length of the period was 4,6mm, and was almost constant for the 8m/min and 10m/min welding speeds.

Welds performed with welding speed 12m/min and higher were in the humping regime and it is possible that the cyclic changes of penetration at speeds between 8m/min and 10m/min are part of a 'pre-humping' phenomenon which evolves into humping at greater speeds.

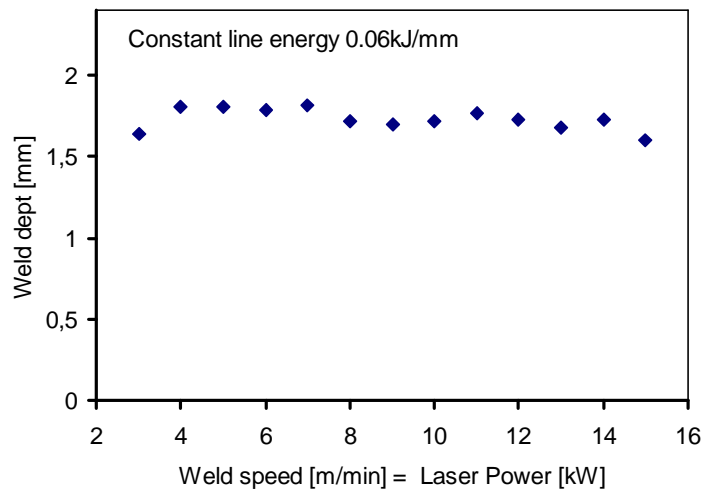


Fig 8. Weld depth measured from cross-cuts.

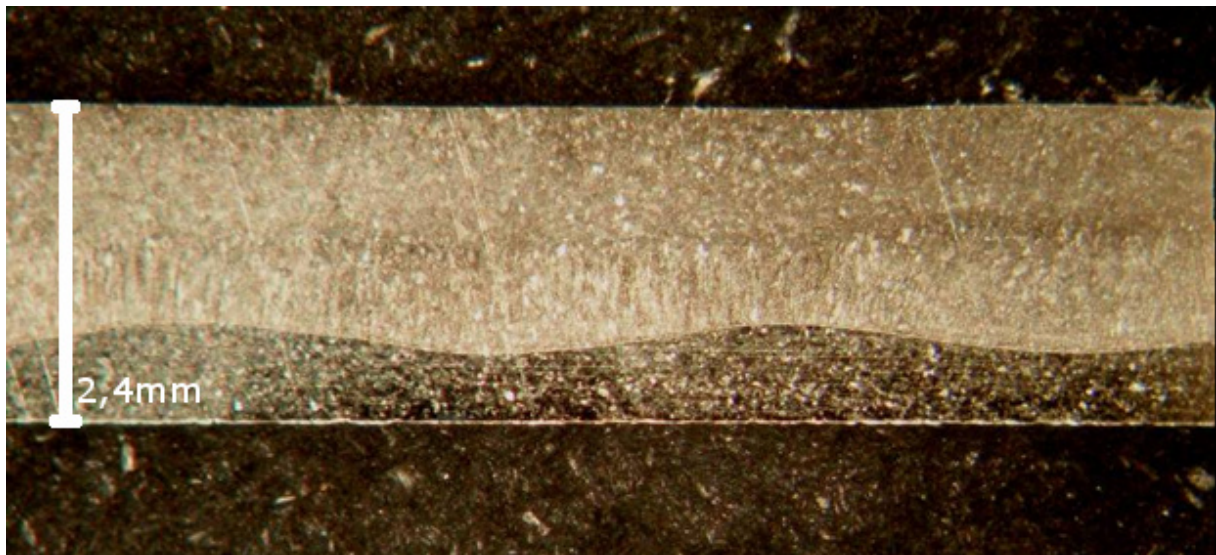


Fig 9. Etched cut along weld. 9kW laser power, 9m/min welding speed (150mm/s)

As soon as the welding process is in the humping regime, large undercuts are created. And the characteristic periodic humps are build up along the centre of the weld.

Fig 10 shows cross sections of three welds of similar line energy but increasing welding speed and laser power. It is clear from these images that the melt becomes progressively more

undercut as the power/speed is increased. At the highest powers and speeds the weld melt pool is not connected to the substrate on either side.

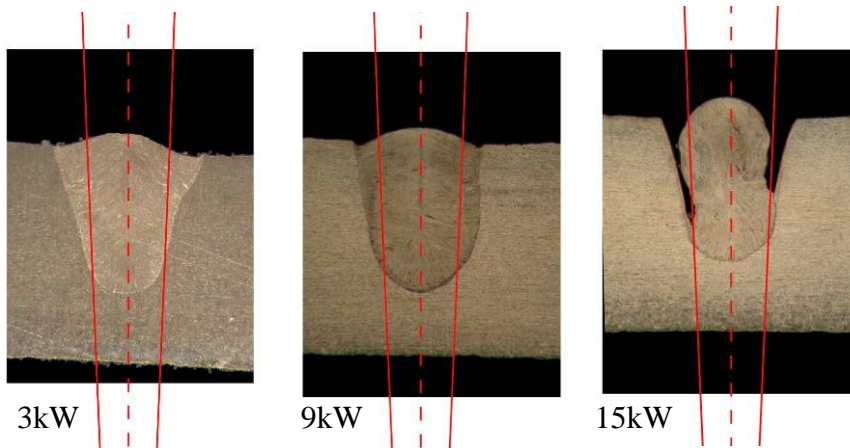


Fig 10. Cross-cuts at different welding speed / laser power.

The 2d-FFT velocity estimation of the downward keyhole front flow from the welds with constant line energy is shown in **Fig 11**. As mentioned earlier the welds with laser power of 12-15kW were completely in the humping regime. In the weld with 3kW, no continuous flow was identified.

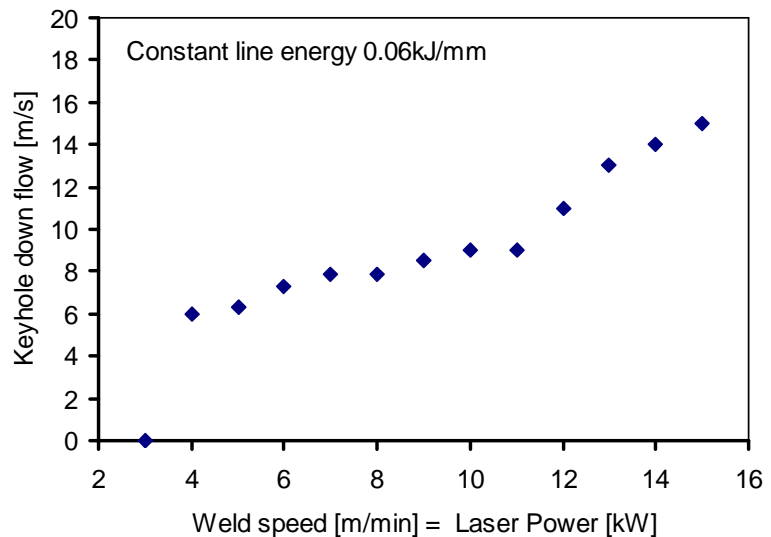


Fig 11. Downward flow during welds with line energy of 0.06kJ/mm

4 Discussion

The high speed video shows that there is a downward motion on the keyhole front during laser keyhole welding at sufficient speed and power. When the laser power is high and the welding speed low, the downward flow is sufficient to eject molten metal away from the bottom of the plate and produce a cut. This cutting action confirms that it is not only waves on the surface that are moving, but there is a substantial flow of molten metal down the keyhole front.

The results presented in **Fig 7** show that the flow velocity is governed by the laser power. Changing the welding speed has no significant influence above a certain speed (50mm/s in our setup). At speeds below this threshold there is a reduction in clearly directed continuous flow, and fluid motion is more random. In this paper only one focal point position was utilized. But it should be noted that a change of focal position changes the power density

distribution which could also change the melt flow velocity. However not enough experiments have been conducted in this area to draw any conclusions yet, so no results are presented in this paper.

Cause of downward flow

The hypothesis from the authors is that, except at the lowest speeds, the keyhole front wall is inclined as in **Fig 12**. Small perturbations in the process initiate bumps in the molten metal. When the laser beam evaporates metal on the top of the bumps a downward recoil pressure is created. The recoil pressure propels the bumps downwards. An increase in laser power will increase the evaporation pressure which leads to an increase in the downward velocity of the molten metal.

The effect of downward and backward flow

As speeds increase the keyhole front wall becomes progressively tilted in the direction of welding ie it becomes less vertical. This increases the backward thrust component of the flow down the keyhole front wall. If the backward flow becomes too high, the result is large undercuts and humping, as seen in **Fig 10** for the 15kW weld.

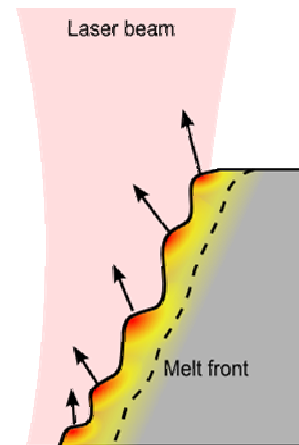


Fig 12. Locally heated bumps with evaporation pressure normal to the surface

5. Conclusions

For stainless steel it has been identified that there is a flow of melt down the leading edge of the keyhole during fibre laser welding. The flow disappears if the welding speed is low.

The speed of this flow is of the order of m/s (in our case between 4 and 25 m/s).

At high welding speed and power, the speed of the flow also increases, and the changing inclination of the keyhole front projects more of this melt flow backwards into the melt pool which follows the laser beam. This can give rise to humping and the lack of attachment of the solidifying melt to the substrate on either side of the weld line.

6 Acknowledgement

This research has been carried out in the FiberTube Advanced project, funded by Jernkontoret - The Swedish Steel Producers' Association, project no. 34013.

References

- [1] Fabbro R.:
Melt pool and keyhole behaviour analysis for deep penetration laser welding, Journal of Physics D: Applied Physics,**43**,0022-3727, p. 445501 (2010)
- [2] Kamimuki K.;Inoue T.;Yasuda K.;Muro M.;Nakabayashi T.;Matsunawa A.:
Prevention of welding defect by side gas flow and its monitoring method in continuous wave Nd:YAG laser welding, Journal of Laser Applications,**14**, p. 136-45 (2002)
- [3] Rai R.;Elmer J.;Palmer T.A.;DebRoy T.:
Heat transfer and fluid flow during keyhole mode laser welding of tantalum, Ti-6Al-4V, 304L stainless steel and vanadium, Journal of Physics D: Applied Physics,**40**,0022-3727, p. 5753 (2007)
- [4] Otto A.;Schmidt M.:
Towards a universal numerical simulation model for laser material processing, Physics Procedia,**5**,1875-3892, p. 35-46 (2010)
- [5] Semak V.V.;Bragg W.D.;Damkroger B.;Kempka S.:
Transient model for the keyhole during laser welding, Journal of Physics D: Applied Physics,**32**,0022-3727, p. L61 (1999)
- [6] Eriksson I.;Gren P.;Powell J.;Kaplan A.F.H.:
New high-speed photography technique for observation of fluid flow in laser welding, Optical Engineering,**49**, p. 100503 (2010)
- [7] DebRoy T.;David S.A.:
Physical processes in fusion welding, Reviews of Modern Physics,**67**, p. 85 (1995)
- [8] Blackburn J.;Allen C.;Hilton P.;Li L.:
Nd:YAG laser welding of titanium alloys using a directed gas jet, Journal of Laser Applications,**22**, p. 71-8 (2010)
- [9] Greses J.;Hilton P.A.;Barlow C.Y.;Steen W.M.:
Plume attenuation under high power Nd:yttrium--aluminum--garnet laser welding, Journal of Laser Applications,**16**, p. 9-15 (2004)
- [10] Weberpals J.; Dausinger F:
Fundamental understanding of spatter behavior at laser welding of steel. Proceedings 27th ICALEO Conference, October 2008, Temecula, CA USA, Paper #704 (2008)